

High-pressure x-ray diffraction measurements on vitreous GeO₂ under hydrostatic conditionsQ. Mei,^{1,*†} S. Sinogeikin,¹ G. Shen,^{1,*‡} S. Amin,² C. J. Benmore,³ and K. Ding⁴¹*HPCAT, Geophysical Laboratory, Carnegie Institution of Washington, Bldg. 434E, 9700 S. Cass Avenue, Argonne, Illinois 60439, USA*²*Department of Chemistry and Biochemistry, Arizona State University, Tempe, Arizona 85287-1604, USA*³*Advanced Photon Source, Argonne National Laboratory, Argonne, Illinois 60439, USA*⁴*School of Metallurgical Engineering, Xian University of Architecture and Technology,**13 Yanta Road, Xian 710055, People's Republic of China*

(Received 19 February 2010; published 20 May 2010)

The x-ray structure factors of vitreous GeO₂ have been measured at pressures up to 15.7 GPa in a laser-perforated diamond anvil cell under hydrostatic conditions using a monochromatic, microfocused high-energy x-ray beam. The results reveal a monotonic increase of the average coordination number of oxygen atoms around Ge with pressure from 4.2(2) at 5.1 GPa to 5.5(3) at 15.7 GPa. The coordination number change suggests that the structural transition range has been extended and pushed to higher pressure under hydrostatic conditions.

DOI: [10.1103/PhysRevB.81.174113](https://doi.org/10.1103/PhysRevB.81.174113)

PACS number(s): 61.05.cp, 61.43.Fs, 62.50.-p

I. INTRODUCTION

Archetypal network-forming glasses such as SiO₂ and GeO₂ have been studied extensively due to both their geological and technological importance.¹⁻¹⁰ At ambient pressure GeO₂ glass is considered to be a structural analog of silica glass because both systems have a continuous three-dimensional network consisting of corner-sharing tetrahedra. GeO₂ glass is of particular interest because the structural transition with pressure can be observed at less severe thermodynamic conditions.^{3,6} It has been suggested that the GeO₂ glass may undergo a transition to metastable high-density form characterized by an average Ge-O coordination number of ~ 5 between 6 and 10 GPa, comprising of a mixture of 4,5 and sixfold polyhedra, before a fully octahedral connected state is formed at high pressure.⁶ However, other densification models have also been proposed.⁷⁻¹⁰ Shanavas *et al.*⁷ performed molecular dynamics (MD) simulations on GeO₂ glass under pressure and found a large number of Ge atoms ($\sim 50\%$ at ~ 7 GPa) are coordinated to five oxygen atoms under high pressure. The computed variation of total coordination shows that there is no unambiguous plateau in the average coordination number at ~ 5 even though the rate of coordination increase is rather small. The MD simulations by Micoulaut *et al.*^{8,9} suggested that the structural modifications with pressure appear to be stepwise and gradually affect the longer-range correlations [manifested by a shift in the first sharp diffraction peak (FSDP)], a reduction in the average bond angle distribution and finally a distortion of the short-range tetrahedral structure. Both simulations show that even up to ~ 30 GPa, the state is not fully octahedrally connected. Hong *et al.* performed density, x-ray scattering, and Raman measurements on GeO₂ glass under high pressure.¹⁰ They observed that both the width of the FSDP and the Raman stretching band of Ge-O-Ge increase with pressure but exhibit changes in behavior at 2.5 and 7.5 GPa, indicating intermediate states exist in the glass before the collapse of local tetrahedral and pentahedral structural units, respectively.¹⁰ Drewitt *et al.*¹¹ investigated the structure of GeO₂ glass at pressures up to 8.6 GPa using neutron diffrac-

tion. They found that Ge-O coordination number increases steadily from 4.0(1) to 4.9(1) as the pressure increases to 8.6(5) GPa, and the corresponding distance increases from 1.73(2) to 1.77(2) Å.

It is found that nonhydrostatic stresses play an important role in the pressure induced amorphization process or pressure induced phase transition for crystalline materials.^{12,13} α quartz, which has been found to undergo pressure-induced amorphization, was found to transform to a monoclinic, crystalline phase when compressed to 45 GPa at room temperature in a (quasi-) hydrostatic, helium pressure medium.¹⁴ α -quartz-type GeO₂ was found to undergo an transition to a monoclinic crystalline phase above 6 GPa at room temperature from *in situ* x-ray diffraction measurements.¹⁵ In GeO₂, the degree of crystallization of the monoclinic P2_{1/c} phase was found to be highly dependent on the hydrostatic conditions provided by the pressure-transmitting medium.¹⁵ The effects of nonhydrostaticity on the glass structure transition under pressure have not been studied extensively. Therefore, we have used a helium medium to study the GeO₂ glass transition under (quasi-) hydrostatic conditions in this work.

In this study, we aim at optimizing the experimental conditions for studying the structural transition in GeO₂ glasses with a focus on the nature of coordination number change as a function of pressure. High energy x-rays from synchrotron radiation were used for large momentum transfer (Q) coverage. A perforated diamond anvil cell (DAC) was used for reducing the background from diamond anvils. The use of a helium medium provided the best possible (quasi-) hydrostatic conditions.

II. EXPERIMENTAL

The GeO₂ glass sample was prepared by melting crystalline GeO₂ powder of high purity grade (99.98%, alpha) using Platinum crucible in an electrical furnace at 1500 °C for 4 h. Then the glass melt was quenched in air. The transparent appearance, along with broad vibrational modes from Raman measurements were used to confirm that the sample is amorphous.

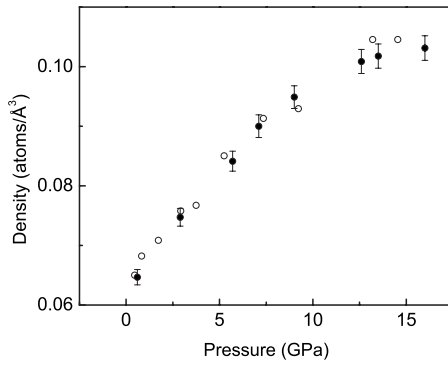


FIG. 1. Densities of GeO_2 glasses as a function of pressure under hydrostatic condition (solid circles are from this work) compared to nonhydrostatic conditions (open circles are from Ref. 10).

The *in situ* high-pressure x-ray diffraction measurements were conducted at the beamline 1-ID at the advanced photon source (APS) using a cryogenically cooled bent double-Laue monochromator¹⁶ with an incident beam of area of $20 \times 20 \mu\text{m}^2$ and high-incident beam energy of 80.0 keV. Pressure was applied to the sample using a symmetrical DAC with a *c*-BN seat at the downstream side, allowing reliable diffraction patterns to be taken in a large solid angle up to a maximum scattering angle 2θ of 24° .¹⁷ The DAC was fitted with 400 μm culet anvils (type I) of length of 2.15 mm and a rhenium gasket (250 μm thickness) was preindented to 40 μm in thickness. A laser-perforated diamond was used at the downstream position to minimize the amount of anvil material in the beam path and thereby the Compton scattering from the DAC, while maintaining a relatively high strength.¹⁸ A sample chamber, 190 μm in diameter, was drilled into the preindented gasket by using a microelectrodischarge machining technique, creating a cavity of $\sim 3 \times 10^{-4} \text{mm}^3$, which housed the glassy GeO_2 . Two ruby balls, each of volume about 10 μm^3 , were placed in the sample container to determine the pressure using the ruby

fluorescence technique.¹⁹ Helium was loaded to the DAC at room temperature by using a high-pressure gas-loading system at GeoSoilEnviroCARS at APS. The DAC was sealed at 2.2 GPa and the gasket hole size shrank from 190 to 120 μm . Helium solidifies at about 12 GPa but offers good quasi-hydrostatic conditions to at least 50 GPa.²⁰

The density of GeO_2 glass was measured as a function of pressure up to 17 GPa using a diamond anvil cell at room temperature under quasi-hydrostatic conditions during a separate run. A flat piece of glass with an area of approximately 5100 μm^2 and thickness of less than 20 μm was surrounded by a helium medium under quasi-hydrostatic conditions up to 17 GPa. Digital images of the sample loaded in the diamond cell were taken with a 3 Mpixel camera (LEICA DFC290) mounted on a stereomicroscope (LEICA MZ16). By integrating the pixels in these digital images, it was possible to measure the change in area of a GeO_2 sample during compression and calculate the densification by relating the change in volume to the change in area via the equation $V/V_0 = (A/A_0)\sqrt{(A/A_0)}$, where V and V_0 refer to the final and initial volumes and A and A_0 refer to the final and initial areas, respectively.^{21,22}

III. RESULTS AND DISCUSSION

The density change of glassy GeO_2 as a function of pressure, P , is shown in Fig. 1, in comparison with the data in Ref. 10. Although it is noticeable that the density increase curves overlap slightly between 6 and 9 GPa under nonhydrostatic conditions,¹⁰ no density plateau has been observed in this study with helium loading. We therefore suggest that the differences between these two studies are not significant and within the error bar range (Fig. 1). It should be pointed out that the density increases by 59% over the pressure range of 0.6–16 GPa.

A partially perforated diamond was used at the downstream position to minimize the amount of anvil material in

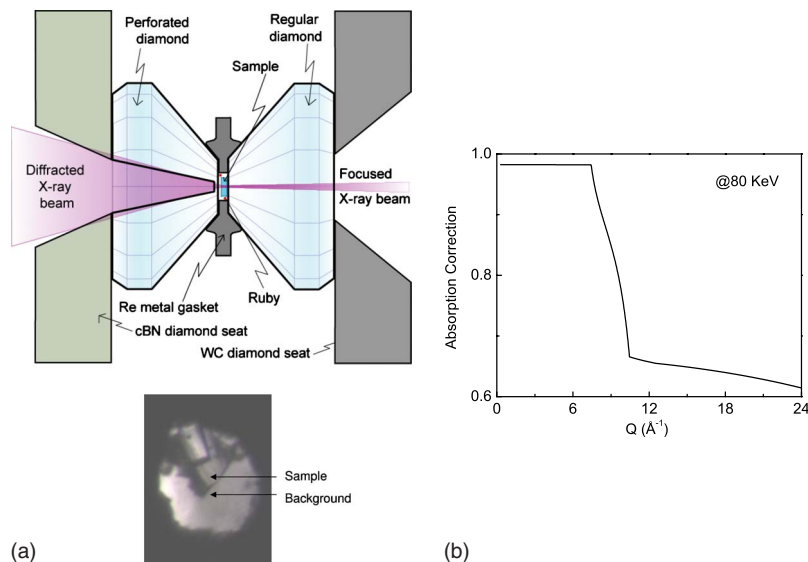


FIG. 2. (Color online) (a) A schematic drawing of the DAC with one partially perforated diamond and a photograph of the sample loaded in the DAC (at 15.7 GPa). (b) Absorption correction curve as a function of momentum transfer.

the beam and thereby the Compton scattering from the DAC. A *c*-BN seat was combined with the perforated diamond to reduce the risk of breaking the diamond although this complicates the absorption correction during data analysis. A schematic drawing of the DAC with one perforated diamond is shown in Fig. 2(a). The amorphous-Si General Electric flat plate area detector was exposed 200 times with each exposure of 16 s to avoid saturation due to the Bragg peaks from the diamonds. The background was collected *in situ* from an area only having helium medium within the gasket which is 20 μm away from the sample location. The contribution from the 20–30 μm thick helium at 80 KeV is negligible. An alternative way for background collection is to take an empty cell x-ray pattern before sample loading and after decompression. A linear combination of these two backgrounds can be used for data reduction at different pressure points. This approach was not used in this experiment because the combination of a partially perforated diamond and a helium medium put the diamonds under risk of breaking at high pressures. In this experiment, the perforated diamond failed catastrophically during the initial step of decompression. The data analysis and corrections were based on Eq. (1) in Ref. 18 and the only term that has been added is the absorption correction from the *c*-BN seat. The Q -dependent absorption correction was calculated based on the geometry of the diamond and the *c*-BN seat and it is shown in Fig. 2(b). It is found that more than 30% of the intensity has been lost due to the absorption from the *c*-BN seat above 10.5 \AA^{-1} .

The x-ray patterns on the sample and background were measured at two spots that were 10 μm away from the center of the hole in vertical direction [see Fig. 2(a)]. The rhenium signals were present in both the sample spectra and the background spectra because the focused x-ray beam had a tail in horizontal direction. In principle, the rhenium signal should be cancelled out completely if the hole remains symmetric and round under pressure. However, the diamond anvil cell was sealed under pressure and the hole shrank to an irregular shape even at low pressures and the asymmetry increased with increasing pressure [see Fig. 2(a)]. A highly focused beam could have solved the problem, but it is very difficult to get the beam completely focused at such high energy.

The x-ray total structure factor $S(Q)$ for vitreous GeO_2 at pressures up to 15.7 GPa are shown in Fig. 3. The dips at 3.00(2), 4.55(2), and 7.18(2) \AA^{-1} arise from the oversubtraction of the rhenium gasket signal in the background data set and these features become more pronounced as the gasket hole shrinks at higher pressure. These dips do not have any significant effects on the total correlation functions in real space because the first and second nearest neighboring Re-Re correlation distances are at 2.74(1) and 3.89(1) \AA , respectively. These features do not overlap with the main peaks from GeO_2 glass. This has been confirmed by manually repairing these dips and Fourier transforming the data to the total distribution function, $T(r)$. The discrepancy in coordination number calculation is less than 0.5% with and without these points. Here we define $T(r)$ as

$$T(r) = 4\pi\rho rG(r), \quad (1)$$

where $G(r)$ is the pair distribution function and it is defined as

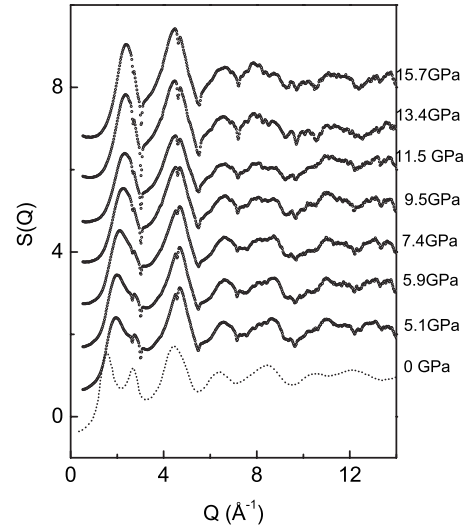


FIG. 3. Measured high-energy x-ray structure factors for GeO_2 glasses at high pressures (the data at ambient pressure is taken from Ref. 29).

$$G(r) = 1 + \frac{1}{2\pi^2\rho} \int_0^\infty [S(Q) - 1] \times \left(\frac{\sin Qr}{Qr} \right) Q^2 dQ, \quad (2)$$

and ρ is total number density.²³

For covalently bonded glassy networks such as GeO_2 , the first sharp diffraction peak at position Q_1 in x-ray diffraction pattern has often been associated with the existence of intermediate range order (IRO), with a periodicity of $2\pi/Q_1$. Earlier experiments suggest that the significant modification of IRO occur in covalently bonded networks under nonhydrostatic pressure, signified by the intensity reduction and the peak shift of the FSDP to higher Q values.^{5,18,24} Several experimental and simulation studies have demonstrated that the densification is accompanied by an overall alteration in the ring sizes and a collapse of void space, which is associated with the change of connectivity among tetrahedral units.^{25–27} As shown in Fig. 3, the x-ray FSDP for GeO_2 glass shifts from 1.57(2) \AA^{-1} at 0 GPa to 2.38(2) \AA^{-1} at 15.7 GPa.^{28,29} However, a reduction of the intensity of the FSDP is not observed as the principle peak gets merged in the FSDP under pressure.

The pressure dependence of the position of the FSDP in the total structure factor is shown in Fig. 4, in comparison with the results obtained by Hong *et al.* and Guthrie *et al.*^{6,10} Our data show a linear increase in Q_1 with pressure up to ~ 10 GPa, which is consistent with a steady collapse of the intermediate range order. The linear slope of Q_1 versus pressure under hydrostatic conditions in this study agrees well with those by Guthrie *et al.* (Fig. 4) but is different to the measurements by Hong *et al.* which occurs more gradually. However based on the data from this work and that from Hong *et al.*, the increase of Q_1 with pressure for glassy GeO_2 flattens above ~ 10 GPa. This is consistent with the extended x-ray absorption fine structure (EXAFS) studies, which shows the EXAFS signal beyond the first Ge-O shell is progressively lost up to 10 GPa.³⁰ In comparison, the Q_1

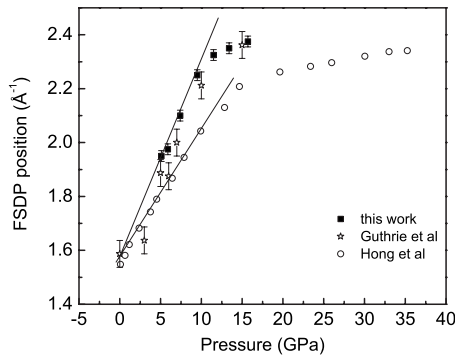


FIG. 4. The pressure dependence of the position of the FSDP in the total structure factor, in comparison with the results obtained by Hong *et al.* and Guthrie *et al.* (Refs. 6 and 10). Lines are guides for eyes.

for SiO_2 glass deviate from the linear line at 15 GPa, where it coincides with the pressure where the short range order structure starts to change i.e., tetrahedra begin to convert to octahedra.³¹ For the GeO_2 glass studied in this work, the conversion of tetrahedra to octahedra starts to occur at ~ 5 GPa. One plausible interpretation of these observations is that as the intermediate range order structural collapse fills up void space it starts to cause the short range order structure to become distorted leading to an increase in Ge-O coordination.

Figures 5(a) and 5(b) show the total correlation functions $T(r)$ for GeO_2 glasses at a series of pressures with and without a Lorch window function applied during the Fourier transformation.³² Spurious truncation ripples are smoothed from the radial distribution functions with the application of a Lorch function, which allows a more accurate identification

of the peak maxima. The average coordination number of oxygen atoms around germanium was subsequently calculated based on the $T(r)$ functions in Fig. 5(a). However, the resolution of the real features is compromised if a window function is applied during Fourier transformation. When a window function is not used we observe how detailed features evolve as a function of pressure but with larger truncation effect peaks [shown in Fig. 5(b)]. The features between 1.5 and 2 Å include a ghost maxima at ~ 1.61 Å, which varies for different pressures since the Q_{cut} is only $\sim 14.2 \text{ \AA}^{-1}$, a Ge-O bond peak at 1.74(2) Å which varies depending on how distorted the tetrahedra become with pressure and a Ge-O bond peak at 1.85(2) Å. The Ge-O distance cannot be determined accurately due to the heavy overlap of these three features. Also, the fraction of the tetrahedra and octahedra cannot be determined by multiple Gaussian fits because they are highly distorted and may not strictly follow a Gaussian distribution under pressure.

However it is observed that the features associated with the Ge-O and Ge-Ge distances in edge shared GeO_6 polyhedra appear to grow continuously in intensity as a function of pressure. The peak at ~ 3.04 Å at 5.1 GPa is assigned to the Ge-Ge correlation distance between corner shared Ge tetrahedra and the peak at ~ 3.32 Å at 15.7 GPa is assigned to Ge-Ge correlation distance between edge shared Ge octahedra. These assignments are made on the basis of crystal structures i.e., the Ge-Ge distance in α -quartz GeO_2 is 3.16 Å and it is 3.30 Å for high pressure phase crystalline GeO_2 .^{33,34} The shortened Ge-Ge correlation distance under pressure is consistent with a significant percentage, of six- and seven-membered rings at ambient pressure converting into smaller rings in the 0–5 GPa range. This is consistent with the results from Raman studies, which show a decrease in intertetrahedral bond angle with pressure.^{35,36} As the

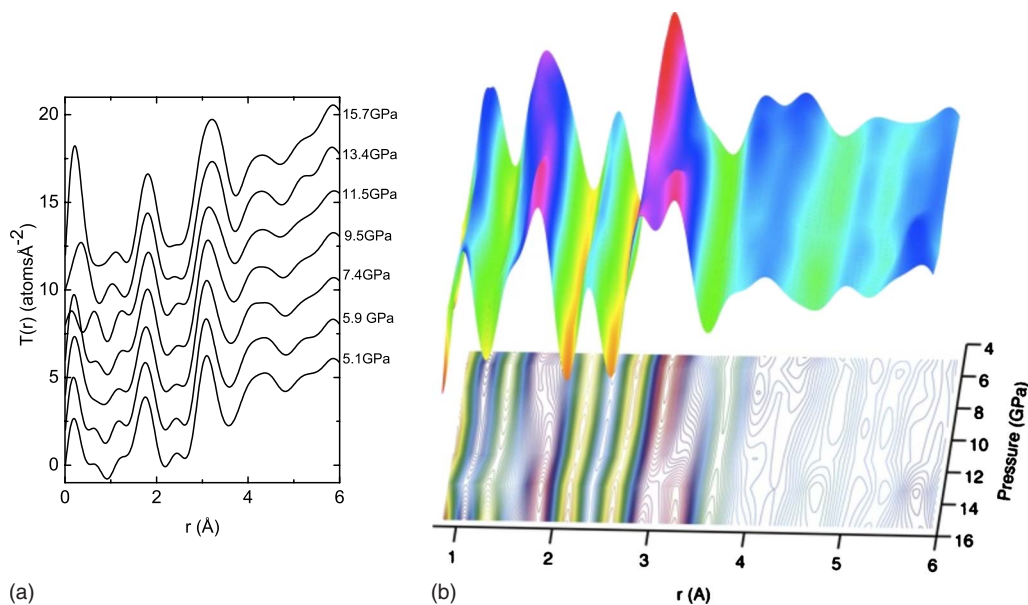


FIG. 5. (Color online) (a) X-ray total correlation functions, $T(r)=4\pi rG(r)$, for GeO_2 glasses at different pressures, corresponding to the Fourier transforms of the curves in Fig. 3 with $Q_{\text{max}}=14.2 \text{ \AA}^{-1}$ and the Lorch window function applied. (b) Surface and contour plot of x-ray total correlation functions for GeO_2 glasses at different pressures, corresponding to the Fourier transforms of the curves in Fig. 3 with $Q_{\text{max}}=14.2 \text{ \AA}^{-1}$ and no window function applied. For α -quartz GeO_2 , Ge-O distance=1.735 Å, and Ge-Ge distance=3.164 Å (Ref. 33). For high-pressure phase GeO_2 , Ge-O distance=1.85 Å, and Ge-Ge distance=3.301 Å (Ref. 34).

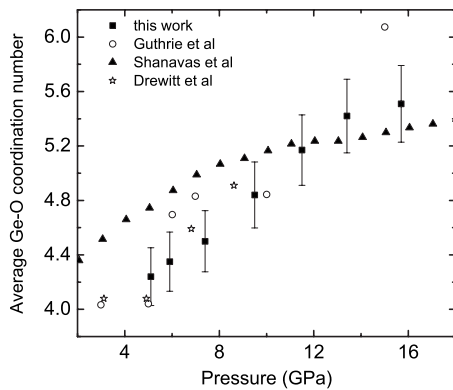


FIG. 6. The coordination numbers were calculated based on $G(r)$'s that Fourier transformed with the Lorch function applied, in comparison with the data from Refs. 6, 7, and 11.

packing of the tetrahedral units becomes denser, the intensity of the Ge-Ge peak associated with the formation octahedra increases continuously as a function of pressure and the first Ge-O peak width broadens with pressure (see Fig. 5).

The average coordination numbers of oxygen atoms around germanium at different pressures has been calculated based on the integrating of the area beneath the Ge-O peak in $G(r)*r^2$ and the density data as shown in Fig. 1. The coordination numbers calculated in this work are shown in Fig. 6, along with the data obtained by Guthrie *et al.*, Shanavas *et al.*, and Drewitt *et al.*^{6,7,11} Shanavas *et al.* performed molecular dynamics simulations on GeO_2 glass under hydrostatic conditions⁷ and predict that the increasing of the Ge-O coordination number slows down once it reaches 5. A plateau in the average Ge-O coordination number around 5 is not observed in our data, although the slope changes slightly at 11.5 GPa. These results are in agreement within the error bars of previous studies.^{6,11} A large number of Ge atoms ($\sim 50\%$ at 7 GPa) are coordinated to five oxygen atoms based on the simulations and a mixture of four-, five-, and six-coordinated polyhedra is a likely scenario during the structural transition. The MD simulations⁷ also suggest that the structure is not fully octahedrally connected at ~ 30 GPa, which is in good agreement with EXAFS study that was performed by Baldini *et al.*³⁷ The results from this study cannot confirm that the glass is fully octahedral; since we only studied the structural changes up to ~ 16 GPa and the transition was not complete.

Marrocchelli *et al.*³⁸ recently attempted to address the controversy over the structure of glassy GeO_2 at high pressure with molecular dynamics simulations using an interaction potential which includes dipole polarization effects. The MD results³⁸ predict a smooth structural transition from a tetrahedral to octahedral network in agreement with this study and find that this is associated with a significant number of pentacoordinated germanium atoms appearing over a wide pressure range. Marrocchelli *et al.* claimed that in the pioneering x-ray study of Guthrie *et al.*,⁶ the authors interpret their data as a very sharp transition from a tetrahedral to octahedral structure starting around 4–5 GPa, which is not the case. The observed changes in the diffraction data at this pressure simply mark the threshold at which the average

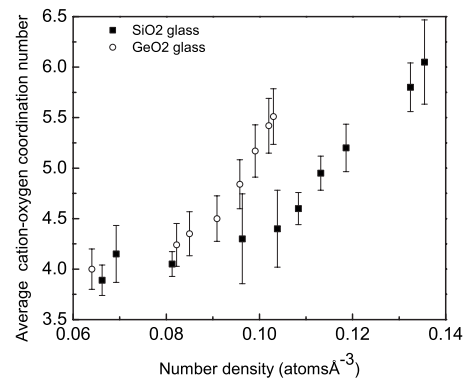


FIG. 7. Comparison of the number density dependence of the coordination number for GeO_2 and SiO_2 glasses (Ref. 31).

Ge-O coordination number starts to increase above 4.

Hong *et al.* suggested that the transition to the octahedral form is completed at 13 GPa and the postoctahedral compression process is active above 15 GPa under nonhydrostatic conditions.¹⁰ Guthrie *et al.* suggested that the glass structure is fully octahedrally connected at 15 GPa, with the Ge-O peak centered at $1.91(2)$ Å.⁶ In this study, the coordination number reaches $5.5(3)$ with the Ge-O peak centered at $1.81(2)$ Å [see Fig. 5(a)] at 15.7 GPa under hydrostatic conditions. Therefore, it is likely that the structural transition has been pushed to a higher pressure and has a broader range under hydrostatic conditions. Similarly, it has been reported that the polyamorphic transition in B_2O_3 glass under both compression and decompression are broad under hydrostatic conditions using energy-dispersive x-ray diffraction.³⁹ The abrupt changes of sound velocities for B_2O_3 glass that had been reported earlier are associated with strongly nonhydrostatic conditions near the sample.^{39,40}

A comparison of the average cation-oxygen coordination number for GeO_2 and SiO_2 is shown in Fig. 7 as a function of atomic number density.²⁹ Both glasses show similar behavior, exhibiting a threshold above which the average coordination number starts to steadily increase. For GeO_2 the threshold is 16% lower than SiO_2 and the rise in coordination number slightly more rapid, reflecting the difference in the repulsion-dispersion terms of the inter-atomic potentials of Ge-O compared to Si-O.⁴¹

IV. CONCLUSIONS

The measured density of vitreous GeO_2 increases smoothly by 59% over the pressure range between 0.6 GPa and 16 GPa and the data agree with the densities published by Hong *et al.*¹⁰ The x-ray structure factors of vitreous GeO_2 have been measured at pressures up to 15.7 GPa in a laser-perforated diamond anvil cell under hydrostatic conditions using a monochromatic, microfocused high-energy x-ray beam. The results reveal a monotonic increase with pressure of the average coordination number of oxygen atoms around Ge from $4.2(2)$ at 5.1 GPa to $5.5(3)$ at 15.7 GPa.

ACKNOWLEDGMENTS

This work was supported by the National Science Foundation under Grant No. EAR-0738852. Vitali Prakapenka, Qiaoshi Zeng, and Peter Lee are thanked for the assistance during the high-energy x-ray experiments. Malcolm Guthrie, Emmanuel Soignard, and Jeff Yarger are thanked for the

helpful discussion during data analysis. We would like to acknowledge GSECARS and COMPRES for providing helium gas loading system. HPCAT is supported by CIW, CDAC, UNLV, and LLNL through funding from DOE-NNSA, DOE-BES, and NSF. APS is supported by DOE-BES, under Contract No. DE-AC02-06CH11357.

*Corresponding author.

†qiang.mei@hpcat.aps.anl.gov

‡gshen@ciw.edu

- ¹C. Meade, R. J. Hemley, and H. K. Mao, *Phys. Rev. Lett.* **69**, 1387 (1992).
- ²J. F. Lin, H. Fukui, D. Prendergast, T. Okuchi, Y. Q. Cai, N. Hiraoka, C.-S. Yoo, A. Trave, P. Eng, M. Y. Hu, and P. Chow, *Phys. Rev. B* **75**, 012201 (2007).
- ³T. Sato and N. Funamori, *Phys. Rev. Lett.* **101**, 255502 (2008).
- ⁴G. Y. Shen, H. P. Liermann, S. Sinogeikin, W. Yang, X. Hong, C.-S. Yoo, and H. Cynn, *Proc. Natl. Acad. Sci. U.S.A.* **104**, 14576 (2007).
- ⁵Y. Inamura, Y. Katayama, W. Utsumi, and K. I. Funakoshi, *Phys. Rev. Lett.* **93**, 015501 (2004).
- ⁶M. Guthrie, C. A. Tulk, C. J. Benmore, J. Xu, J. L. Yarger, D. D. Klug, J. S. Tse, H.-k. Mao, and R. J. Hemley, *Phys. Rev. Lett.* **93**, 115502 (2004).
- ⁷K. V. Shanavas, N. Garg, and S. M. Sharma, *Phys. Rev. B* **73**, 094120 (2006).
- ⁸M. Micoulaut, *J. Phys.: Condens. Matter* **16**, L131 (2004).
- ⁹M. Micoulaut, Y. Guissani, and B. Guillot, *Phys. Rev. E* **73**, 031504 (2006).
- ¹⁰X. Hong, G. Shen, V. B. Prakapenka, M. Newville, M. L. Rivers, and S. R. Sutton, *Phys. Rev. B* **75**, 104201 (2007).
- ¹¹J. W. E. Drewitt, P. S. Salmon, A. C. Barnes, S. Klotz, H. E. Fischer, and W. A. Crichton, *Phys. Rev. B* **81**, 014202 (2010).
- ¹²K. J. Kingma, C. Meade, R. J. Hemley, H. K. Mao, and D. R. Veblen, *Science* **259**, 666 (1993).
- ¹³J. W. Watson and S. C. Parker, *Philos. Mag. Lett.* **71**, 59 (1995).
- ¹⁴J. Haines, J. M. Leger, F. Gorelli, and M. Hanfland, *Phys. Rev. Lett.* **87**, 155503 (2001).
- ¹⁵J. Haines, J. M. Leger, and C. Chateau, *Phys. Rev. B* **61**, 8701 (2000).
- ¹⁶C. D. Martin, S. M. Antao, P. J. Chupas, P. L. Lee, S. D. Shastri, and J. B. Parise, *Appl. Phys. Lett.* **86**, 061910 (2005).
- ¹⁷G. Shen, V. B. Prakapenka, M. L. Rivers, and S. R. Sutton, *Phys. Rev. Lett.* **92**, 185701 (2004).
- ¹⁸Q. Mei, C. J. Benmore, E. Soignard, S. Amin, and J. L. Yarger, *J. Phys.: Condens. Matter* **19**, 415103 (2007).
- ¹⁹J. D. Barnett, S. Block, and G. J. Piermarini, *Rev. Sci. Instrum.* **44**, 1 (1973).
- ²⁰K. Takemura, *J. Appl. Phys.* **89**, 662 (2001).
- ²¹K. H. Smith, E. Shero, A. Chizmeshya, and G. H. Wolf, *J. Chem. Phys.* **102**, 6851 (1995).
- ²²C. Meade and R. Jeanloz, in *High Pressure Research in Mineral Physics*, edited by M. H. Manghnani and Y. Syono (American Geophysical Union, Washington, D.C., 1987), p. 41.
- ²³S. Susman, K. J. Volin, D. G. Montague, and D. L. Price, *J. Non-Cryst. Solids* **125**, 168 (1990).
- ²⁴Q. Mei, C. J. Benmore, R. T. Hart, E. Bychkov, P. S. Salmon, C. D. Martin, F. M. Michel, S. M. Antao, P. J. Chupas, P. L. Lee, S. D. Shastri, J. B. Parise, K. Leinenweber, S. Amin, and J. L. Yarger, *Phys. Rev. B* **74**, 014203 (2006).
- ²⁵R. A. B. Devine and J. Arndt, *Phys. Rev. B* **35**, 9376 (1987).
- ²⁶Y. Inamura, M. Arai, M. Nakamura, T. Otomo, N. Kitamura, S. M. Bennington, A. C. Hannon, and U. Buchenau, *J. Non-Cryst. Solids* **293-295**, 389 (2001).
- ²⁷W. Jin, R. K. Kalia, P. Vashishta, and J. P. Rino, *Phys. Rev. B* **50**, 118 (1994).
- ²⁸The diamond anvil cell was closed under pressure and therefore the structure factor at ambient condition was not measured. The structure factor from Ref. 29 at ambient condition is shown in Fig. 3 as a reference.
- ²⁹S. Kohara and K. Suzuya, *J. Phys.: Condens. Matter* **17**, S77 (2005).
- ³⁰M. Vaccari, G. Aquilanti, S. Pascarelli, and O. Mathon, *J. Phys.: Condens. Matter* **21**, 145403 (2009).
- ³¹C. J. Benmore, E. Soignard, S. A. Amin, M. Guthrie, S. D. Shastri, P. L. Lee, and J. L. Yarger, *Phys. Rev. B* **81**, 054105 (2010).
- ³²E. Lorch, *J. Phys. C* **2**, 229 (1969).
- ³³J. Haines, O. Cambon, E. Philippot, L. Chapon, and S. Hull, *J. Solid State Chem.* **166**, 434 (2002).
- ³⁴K. Shiraki, T. Tsuchiya, and S. Ono, *Acta Crystallogr., Sect. B: Struct. Sci.* **59**, 701 (2003).
- ³⁵D. J. Durben and G. H. Wolf, *Phys. Rev. B* **43**, 2355 (1991).
- ³⁶C. H. Polsky, K. H. Smith, and G. H. Wolf, *J. Non-Cryst. Solids* **248**, 159 (1999).
- ³⁷M. Baldini, G. Aquilanti, H.-k. Mao, W. Yang, G. Shen, S. Pascarelli, and W. L. Mao, *Phys. Rev. B* **81**, 024201 (2010).
- ³⁸D. Marrocchelli, M. Salanne, and P. A. Madden, *J. Phys.: Condens. Matter* **22**, 152102 (2010).
- ³⁹V. V. Brazhkin, Y. Katayama, K. Trachenko, O. B. Tsiok, A. G. Lyapin, E. Artacho, M. Dove, G. Ferlat, Y. Inamura, and H. Saitoh, *Phys. Rev. Lett.* **101**, 035702 (2008).
- ⁴⁰J. Nicholas, S. Sinogeikin, J. Kieffer, and J. Bass, *Phys. Rev. Lett.* **92**, 215701 (2004).
- ⁴¹M. Micoulaut, *Chem. Geol.* **213**, 197 (2004).